Circuit Transients due to Arcs on a High-Voltage Solar Array

Roger N. Metz*
Colby College, Waterville, Maine

A simple analytical model has been developed to estimate the effects of negative bias arcs on solar-array power system performance. Solar cell circuit characteristics, plasma conduction to interconnects, stored charge at interconnects and power system loading are modeled approximately by a linear, lumped-element, transient circuit defined with reference to a chosen solar array operating point. Both the thermal ion and ram ion cases are considered. Numerical results for the typical case of a 508-V array consisting of 1000 × 1500, 2 × 2 cm silicon solar cells operating at 80% power are given. The model predicts that such an array is expected to float with about 92% of its area below plasma ground. Arcs incident on the negative terminal of amplitudes as great as 200 A are predicted to produce common mode transients of the negative terminal no greater than about 200 V and differential transients across a resistive load no greater than 1/10 this value. Arcs of substantially less than 100 A amplitude produce small common-mode transient amplitudes and quite negligible differential transient amplitudes.

Nomenclature

A = plasma current collecting area of a solar cell
C = interelectrode capacitance of a solar cell
C_p = plasma capacitance of a solar cell to its surroundings
$C+, C-$ = total plasma capacitances from terminals to plasma ground
C_0 = MC/N, total panel interelectrode equivalent capacitance
E_0 = kinetic energy of ram ions
i = current through a solar cell, the quiescent value of which is i_0
$i_s(t)$ = arc current injected at $V-$
I = total current through the solar array
I_0 = arc current amplitude
J_s = $0.5n_s(2kT_s/\pi m_s)^{1/2}$, the ambient plasma thermal current density
K = arc current rise-time multiplier
M = number of chains of solar cells placed in parallel in the array
m_s = mass of a particle of species, s
N = number of cells in a chain in the array
n_s = number density of particle species, s
p = Laplace transform of $i_s(t)$
$q+, q-$ = Laplace transforms of $v+$ and $v-$
R_L = load resistance placed across an array
$R+, R-$ = total equivalent plasma resistances from terminals to plasma ground
T_s = thermal temperature of particles of species, s
T = arc current fall-time constant
V_T = output terminal voltage of the array, the quiescent value of which is V_T°
$V+, V-$ = voltages of panel terminals relative to plasma ground
$v+, v-$ = transient voltages of panel terminals
v_d = transient voltage difference across the load, i.e., $v+ - v-$
$v(t)$ = transient voltage time function
$V(z)$ = spatial voltage distribution on a chain of cells
Z_p = impedance per cell of the parallel combination of C_p with a plasma conductance
z_0 = the point on a chain at which $V(z_0)$ is zero
α_s = e^2J_sA/kT_s, the thermal plasma conductance of species, s, to an interconnect
α_r = $e^2An_i(2/m_iE_0)^{1/2}$, the conductance to an interconnect due to ram ions
γ = $1 - z_0/N$, the fraction of an array floating above plasma ground
δ = the plasma split parameter
ϵ = the voltage drop across a single cell, the quiescent value of which is ϵ_0
λ_1, λ_2 = solution time constants
λ = $(\rho\alpha)^{1/2}$, the voltage function scale length
ρ = $|d\epsilon/di|$, the dynamic resistance of a cell, the quiescent value of which is ρ_0

Presented as Paper 85-0385 at the AIAA 23rd Aerospace Sciences Meeting, Reno, NV, Jan. 14-17, 1985; received Jan. 28, 1985; revision received Nov. 18, 1985. Copyright © American Institute of Aeronautics and Astronautics, Inc., 1985. All rights reserved.

*Professor of Physics, Department of Physics and Astronomy.

I. Introduction

LABORATORY and flight tests of small, externally biased solar cell arrays show that arcs occur on or near negatively biased solar cell interconnects exposed to plasmas typical of low earth orbit (LEO).[1-4] The voltage threshold of these arcs appears to lie several hundred volts below the plasma ground potential. The large solar arrays desired for future space missions in LEO will have areas operating at voltages more negative than this threshold, if their terminal voltages are sufficiently high.[5] This is especially true if the arrays are permitted to float electrically in the space plasma. Negative bias arcing is a threat to the operation of such arrays if it can be shown that unacceptable electrical transients in the power system due to arcing cannot be avoided. Conversely, arcing may be tolerated if transients and other arc effects are found to be or can be made minimal.

To estimate the severity of transients produced by negative bias arcs, a circuit model of a simple solar array power system has been developed. It shows approximately how load transients due to arcs on an array in LEO depend upon plasma parameters, stored charge, solar cell behavior and arc characteristics. Suitable linearizations permit a completely analytical solution to be obtained in the time domain.

The model is current driven. Current pulses are injected at the negative end of an illuminated and loaded solar array that is in prior electrical equilibrium with the plasma. A pulse causes a positive, common-mode voltage transient of the array circuit relative to the plasma and perturbs the solar cell currents and voltages so as to produce a transient across the load.

The size of this transient depends in part on the operating points of the solar cells. In this paper we assume operation on the high voltage side of the maximum power point where the internal dynamic resistance of the cells is low. Operation at other points can be accommodated by the model but is expected to result in much larger voltage transients. (See Secs. II and V.)

Electrical equilibrium prior to an arc is established by the balance of ion and electron currents to an array. A parasitic dc power loss results, which has been treated elsewhere for the case of much higher terminal voltages than those used here.[6] At higher voltages, e.g. kilovolts, the parasitic currents through individual cells force some cells into current saturation, with a resulting sharp collapse of the solar panel terminal voltage. The linear model presented here restricts itself to much less intense parasitic currents and thus does not apply directly to the kilovolt regime.

Several features of the model establish it as a worst-case analysis. First, the arc injection point is placed at the negative end of the array where it is expected, theoretically, to cause larger transients than if placed at more positive points. Second, the spatial distribution of the plasma interaction with the array is approximated by lumped circuit elements arranged to allow upper-bound estimates of load transients. Third, the load is assumed to be purely resistive. Filtering expected to be included in actual power system loads is withheld. These features permit a rather simple model to be made, one that is useful for probing the space of arc current parameters yielding acceptable load transients on a given array under various conditions.

II. Solar Cell and Solar Array Characteristics

A solar array consisting of M parallel chains of matched solar cells is assumed. Each chain contains N cells wired in series and is connected to the other chains at its ends. Arcs injected at one end of the chains cause equal voltage distributions along them. Therefore, cross wiring between adjacent points of the chains is omitted. Further, model linearity requires that the solar cells not be permitted to depart greatly from their quiescent operating points during a transient. Limiting the arc current amplitude achieves this and makes modeling of reverse biasing, short- and open-circuiting of solar cells and diode protection unnecessary.

If the array is illuminated and loaded so that each cell operates at quiescent voltage and current, ϵ_0 and i_0, then the terminal voltage, V_T°, is $N\epsilon_0$, the output current is Mi_0, the output power is $MN\epsilon_0/i_0$ and the load resistance, R_L, is $N\epsilon_0/Mi_0$. For small fluctuations about the operating point, the terminal voltage is given by

$$V_T = V_T^\circ - \rho_0(I - Mi_0) \tag{1}$$

where $\rho_0 = N\rho/M$. In the model, transient currents are confined to those for which Eq. (1) is a good approximation.

The characteristic for a silicon solar cell may be approximated by the function $\epsilon(i) = a(\ln(b-1)) + c$ where, for a 2×2 cm cell at normal operating temperature under full solar illumination, the values $a = 40$ mV, $b = 132$ mA, and $C = 355$ mV, apply.[7] At full power, an array of such cells having $N = 1000$ and $M = 1500$ produces 82 kW at 450 V with $R_L = \rho_0 = 2.5\ \Omega$. At the high-voltage, 80% power point, which is a typical operating point used for model calculations, the array produces 66 kw of power at 508 V with $R_L = 4\ \Omega$ and $\rho_0 = 0.6\ \Omega$. Operation on the high-current side of maximum power should be avoided in real power systems if large arcs are expected. (See Sec. V.) These array parameters have been chosen to model terminal voltages beyond, but not orders of magnitude beyond, those already flown in space while providing for the production of power at levels anticipated to be required by satellites as large as the proposed Space Station.

A silicon solar cell has an internal capacitance that appears in parallel with ρ. For 2×2 cm silicon cells, $C \approx 0.02$ farad. Thus the impedance due to C becomes important, as compared with ρ, only for pulses lasting about a microsecond or less. Although such short pulses are infrequently seen in laboratory tests, pulses with very short rise times do occur. To model their responses correctly, C must be included.

III. Plasma Interactions

A. Plasma Current Collection

The plasma environment used in this paper is that of the ionosphere near 400 kilometers altitude.[8] Plasma densities in this region rise to 10^5 or 10^6 cm^{-3} and electron and ion mean thermal energies are a few tenths of an electron volt. The ions are O^+, predominantly. Both the Debye length and the electron gyroradius are greater than a centimeter. The electron plasma frequency exceeds 1 MHz.

A solar array placed in such an environment draws current from the plasma to the exposed metallic interconnects. Inasmuch as the interconnects are small compared to the Debye length and electron gyroradius, one might expect orbit-limited Langmuir probe theory to give an adequate estimation of current collection from the plasma. For electrons, this theory predicts currents to a sphere at voltage V, proportional to the collecting area, the electron thermal current density and the factor $(1 + eV/kT)$. Ion collection in this theory is somewhat more involved.[9]

Experimentally the situation is not so simple. Whereas currents to negatively biased interconnects appear to vary roughly linearly with voltage, those to positively biased interconnects are highly non-linear. They vary as $(V - V_0)^p$ where $p \approx 1/2$ at low voltage, $p > 1$ in a "snap-over" region[1] where secondary emission effects on the cover slides become important and $p \approx 1$ at high voltage. However, since snap-over is known experimentally to require seconds to develop, it is unlikely to play a role in the plasma response to the micro- and millisecond arcs expected. Thus the voltage dependence of electron collection may be much more slowly varying on these time scales than is indicated by the quasi-static measurements in which snap-over is seen. The exact dependence is not yet well understood experimentally.

To make progress toward an analytical model, simplifying assumptions regarding plasma current collection must be made. The most helpful is that both electron and ion plasma currents are ohmic, i.e., proportional to voltage. Such currents are characterized by conductances α that depend on the properties of the ambient plasma and on the collecting area per cell. This is the equivalent of orbit-limited, spherical Langmuir probe collection in a thermal plasma with $eV \gg kT$. Since $eV \gg kT$ almost everywhere on a high voltage array in LEO, the ohmic assumption treats ion collection realistically but ignores electron snap-over.

We will assume for species, s, (electrons or O_+ ions) that:

$$I_s = \alpha_s V \tag{2}$$

The plasma is assumed to be Maxwellian. Typical values of the parameters used in the model are: $n_e = n_i = 4\times 10^5$ cm^{-3}, $kT_e = 0.2$ eV $= 2$ kTi, and $A = 1$ cm^2. Then $\alpha_e = 2.4\times 10^{-6}$ mho for the electrons and $\alpha_i = 2\times 10^{-8}$ mho for the ions.

In solar array orientations where ram ion currents to negative interconnects dominate the thermal ion currents, the above formulation requires adjustment. It may be assumed that ion collection is then given by spherical Langmuir probe theory in a streaming plasma in the limit where $eV \gg E_0$. E_0 is the ion ram energy. Thus:

$$I_r = \alpha_r V \tag{3}$$

The ram ion energy for O^+ at 400 km is about 5 eV. This value gives $\alpha_r = 10^{-8}$ mho. Thus, for this case, ram ion collection is not radically different in magnitude than thermal ion collection, and numerical results for this case will not be given.

The ohmic approximation employed here rests much more for its justification on test results with segments of actual solar panels[1] than on theoretical calculations for particular geometries as worked out by others.[10] This is because the geometry of a solar panel is very complex and analytical formulas for collection to such a structure are very hard, if in fact possible, to develop. In any case, the spirit of the present work is that of a rough look at collection in relation primarily to transient behavior within a linear and therefore calculable treatment. The treatment of ions by thermal collection is adopted here to aid calculation, although one can see in Appendix A that at least the current balance conditions prior to an arc are fairly insensitive to absolute current collection magnitudes. Once balance is achieved, transients tend to depend more on the arc currents than on the simultaneous plasma current collection.

B. Stored Charge

The several parts of a solar cell in an array are capacitively coupled to each other and to the surrounding plasma. Substrate-to-cover slide, cover slide-to-plasma sheath and interconnect-to-sheath capacitances in series/parallel combination form an equivalent capacitance per cell, *Cp*. An estimate of this capacitance lies in the range 1-200 pF for standard 2×2 silicon cells. The low value is approximately the capacitance to space to a sphere having area equal to that of one interconnect. The high value is the capacitance of a 2×2 cm cover slide to its substrate. Which of these limits dominates *Cp* depends on whether a cover slide can maintain itself near the plasma potential during an arc by charging from the plasma. If so, *Cp* tends toward th higher limit. Because experimental values are not yet well known, the present calculations draw upon the whole range of *Cp*.

C. Floating Equilibrium

On a self-biased solar array in electrical equilibrium with the space plasma, the electron vs ion current balance condition determines what fraction of the array lies above the plasma potential and what fraction below. Those areas above the plasma potential collect electrons and those below collect ions, almost exclusively. A transition region extending a few times kT_e exists on either side of plasma ground, but this region of mixed collection comprises such a small area of a 500-V array as to contribute negligably to the overall plasma current collection. In the ohmic collection approximation, the conductances, α_e and α_i, determine how the array floats electrically. For the values of α_e and α_i given in Sec. III A, an array will float with about 8% of its area positive. (See Appendix A.)

During an arc, while individual cells are being driven positive in voltage, it is expected that a cell's conductance jumps from α_i to α_e as the cell passes the plasma potential and back again on the negative swing. Unfortunately, such voltage-dependent conductance switches are beyond the scope of the present work. In this model, once floating equilibrium is established and all conductances determined prior to an arc, they are not permitted to change. By using electron conductances somewhat greater than those expected physically, however, it is possible to partially explore the consequences of conductances switching and the resulting enhanced electron collection during an arc.

IV. Equivalent Circuits

A. Transients Response of a Chain of Cells

Figure 1 shows a transient circuit for a single chain of solar cells. An arc current injected at $V-$ flows toward $V+$ and the load, while leaking out to the plasma sheath along the way. The load transient is developed as the sum of the voltage transients across the cells due to the current transients through them.

Since current flowing in a chain toward V+ is diminished by leakage to the plasma sheath, cell voltage transients also diminish in this direction. Thus, if all the impedances, *Zp*, where placed in parallel at $V+$, an overestimate of the load transient would result because all the cells would see the maximum current. Similarly, placing all of the impedances at $V-$ would result in no load transient. These two cases bound the actual, uniform distribution case. An appropriate mixture of these cases approximates the actual one.

Using a mixture of the bounding cases results in a considerable simplification of the plasma interaction circuits. The impedances in each chain are split into two groups, one placed at $V-$ and the other at $V+$, and the groups combined in parallel at each terminal. A "plasma split" parameter δ adjusts the relative numbers of impedances at each terminal while keeping the whole constant. (See Appendix A.) Ranging this parameter permits continuous variation from one bounding case to the other. Figure 2 shows the mixed-case circuit for a single chain of cells.

B. Solar Array Equivalent Circuit

Figure 3 shows the resultant solar array power system transient circuit used in the model. $R+$, $R-$, $C+$, and $C-$ are plasma interaction components whose values are determined as described in Appendix A.

As seen in Appendix B, the terminal transient voltages $v+$ and $v-$ satisfy a set of coupled, first-order differential equations with the arc pulse $i_s(t)$ As current driver. The equations can be solved for arbitrary $i_s(t)$ by the method of Laplace transforms. With $i_s(t) = I_0[\exp(-t/T) - \exp(-Kt/T)]$, the time-domain solutions have the form

$$v(t) = B_1\exp(-Kt/T) + B_2\exp(-t/T) + B_3\exp(\lambda_1 t) + B_4\exp(\lambda_2 t) \quad (4)$$

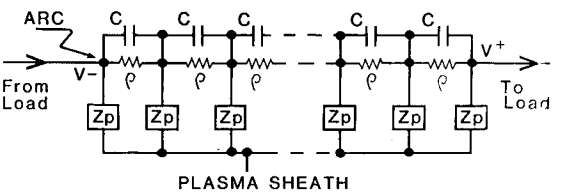

Fig. 1 Cell chain transient circuit.

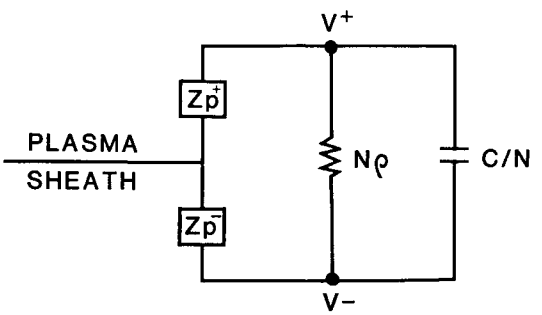

Fig. 2 Mixed-case single chain.

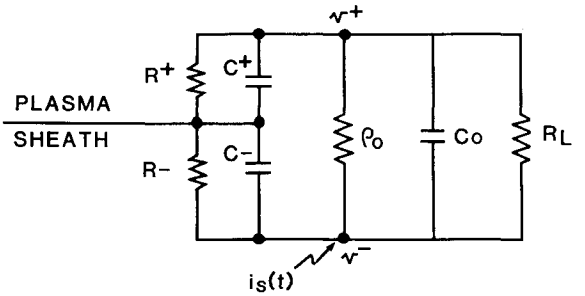

Fig. 3 Array transient circuit.

where B_1---B_4, λ_1 and λ_2 are functions of the circuit parameters and of I_0, K and T. With $K>1$, the driving current pulses have approximately the same time dependence as do arcs seen in laboratory tests.

Although an alternate parameterization of the arcs using an R-L-C series circuit is possible, the I_0, T and K parameterization is more directly comparable to experimental measurements.

V. Results and Discussion

Figures 5-8 show typical numerical results produced by the model. In the figures, $v-$ is the voltage transient amplitude at the negative end of the array and v_d is the load transient amplitude. The values, $N=1000$, $M=1500$, $K=5$, $\alpha_e=2.4\times10^{-6}$ mho and $\alpha_i=2\times10^{-8}$ mho apply throughout. Q is the total charge released, i.e., the integral of $i_s(t)$. I_0, the arc current amplitude, is limited to 200 A to insure the validity of the solar cell characteristic linearization. (See Sec. II).

Figure 4 shows the first-quadrant solar cell characteristic curve used. Operating points for various fractions of maximum power are shown. The sharply increasing negative slope to the right of the maximum power operating point suggests that transient amplitudes per unit arc current should be larger in this region than they are at operating points to the left of the maximum power point where the slope, and hence the dynamic resistance, is smaller. Figure 5, which shows transient voltage amplitudes as a function of operating power for typical conditions, bears this out. There is a factor of almost three between values of v_d at the 90% points on either side of maximum power. This shows that transient amplitudes can be reduced significantly by operating on the high-voltage side of maximum power.

Amplitudes shown in Fig. 6-8 have been calculated assuming operation at 80% power on the high-voltage side. One sees in Fig. 4 that solar cell linearization is a good approximation at this operating point if cell current transients are kept below about 30 mA. $I_0<200$ A achives this.

Figure 6 shows the effect of the "plasma split" parameter, δ. $\delta=1$ corresponds to $C-=1/R-=0$; and $\delta=0$, for which v_d vanishes as it should, corresponds to $C+=1/R+=0$. (See Appendix A.) One sees that amplitudes trend gently downward with decreasing δ and then vary sharply when δ is small. This is because the equilibrium electron conductances are concentrated in a small region near $V+$ where they are all assigned when δ is large. Large values of δ redistribute only the

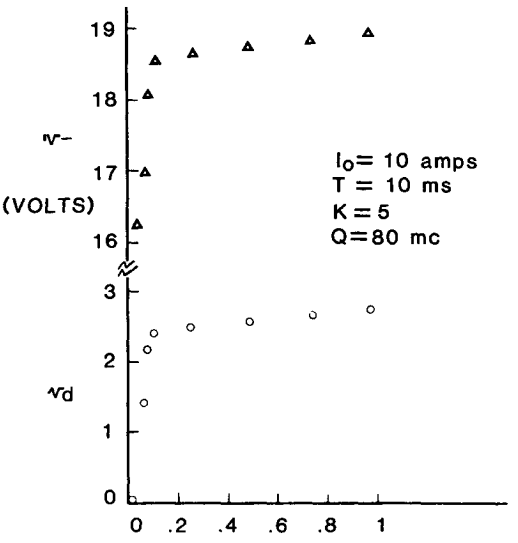

Fig. 6 Transient amplitudes vs δ.

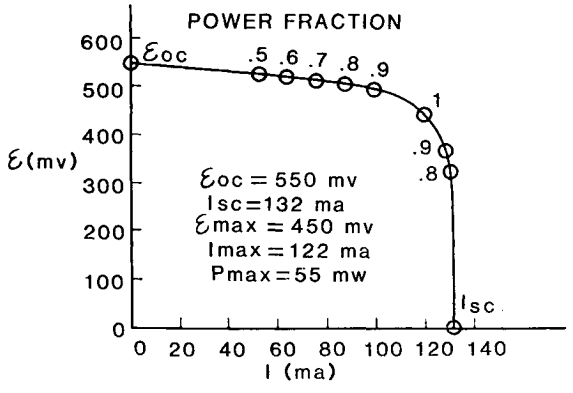

Fig. 4 Solar cell characteristic.

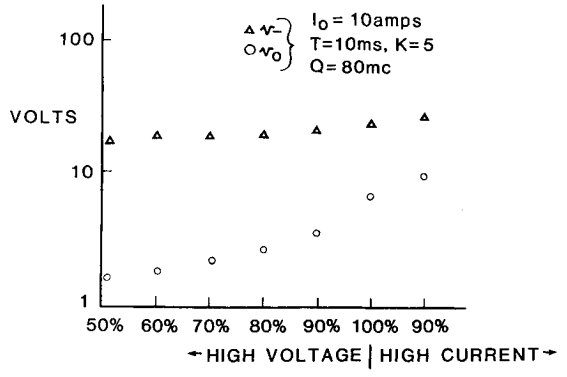

Fig. 5 Transient amplitudes vs maximum power fraction.

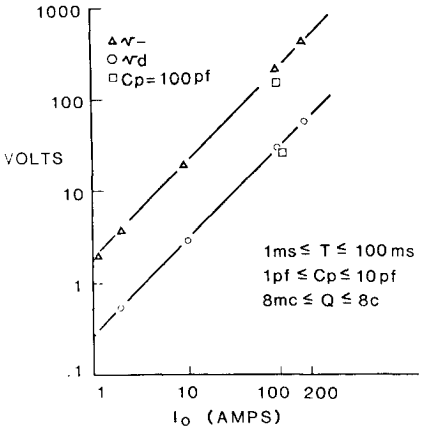

Fig. 7 Transient amplitudes for T in *ms*.

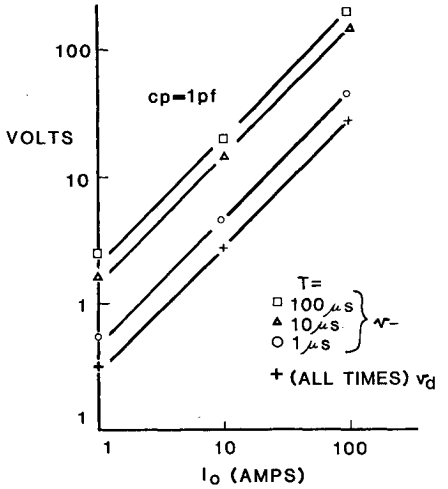

Fig. 8 Transient amplitudes for T in μs.

much weaker ion conductances, leaving the conductances at $V+$ constant. Only when δ becomes less than about .08, which is the fraction of the array initially floating positive, do the large electron conductances at $V+$ begin to shift to $V-$ and cause distributional effects to be seen in the transients.

Figures 7 and 8 show results for two regions of T, the arc pulse fall-time constant. The linear variation with I_0 merely reflects that the solutions are explicitly proportional to I_0. In Figure 7, $v-$ and v_d are seen to be nearly proportional to I_0, with little dependence on T and Cp. This is because T is much larger than circuit time constants, e.g., $R+C+$ or C_0R_L, so the circuit acts mainly like a series pair of resistors driven by $i_s(t)$. In Fig. 8, however, where T is of the order of $R+C+$, some dependence on T is seen in $v-$.

The values of v_d in Figs. 7 and 8 show consistently the relation $v_d/I_0 \approx 0.2\ \Omega$. This means that, for the present array parameters, load transients equal in amplitude to only 8% of the terminal voltage are produced by arcs of 200 A amplitude. Such arcs need only last 0.5 ms in order to transfer 80 mc of charge from an array to the plasma. This amount of charge is expected to be stored on a 1000×1500 cell array operating at 508 V and floating electrically in LEO.

VI. Conclusions

The model presented here is intended to provide a simple means for estimating the transient response of high voltage solar array in LEO to negative bias arcs. By linear approximations, both for the plasma interactions and the solar cell characteristics, an analytical formulation has been made possible. The model is a first step toward more complex analytical and numerical analyses of solar array transients behavior.

An especially needed addition to the model is an independently determined current/voltage characteristic for negative bias arcs. Introducing this to the circuit equations would permit determination of current and voltage transients free of arbitrary parameters. Without it, the model can calculate results only for given pulses. For the special conditions treated, pulses within the limits of the linear approximations of the model are not found to cause clearly unacceptable load transients. Estimation of the effects of stronger arcs awaits a nonlinear analysis.

Even if arc current amplitudes are small enough to cause only negligible single transients, many small arcs might combine to form an essentially continuous discharge. This could clamp the negative end of an array at or near the arc voltage threshold, which is a few hundred volts negative. The resulting enhanced electron collection due to snap-over at the positive end of a high voltage array could cause significant power losses. (See Sec. III A.) This effect needs to be studied further.

Appendix A

Calculation of Floating Equilibrium

For a chain with as many as 1000 cells, the voltage distribution, V, along the chain may be approximated by a continuous function of position. If $\epsilon(i)$ is the current/voltage characteristic of a cell and z locates a point in the chain, then

$$\frac{d^2V}{dz^2} = \frac{d\epsilon}{di}\frac{di}{dz} \qquad \text{for} \qquad 0<n<N \tag{A1}$$

Let the point z_0 divide the chain into ion and electron collection regions. Thus $V(z_0)$ is the plasma potential, here taken to be zero. For ion collection at $z<z_0$, one has $V<0$ and $di = -\alpha_i V dz$ in the ohmic approximation. For electron collection at $z>z_0$, one has $di = -\alpha_e\ Vdz$ and $V>0$. α_i and α_e are defined as in Sec. III A. If the slight variation of cell operating point along the chain is ignored, the cells have a common dynamic resistance, $d\epsilon/di = -\rho$. Substituting these expressions into Eq. (A1) yields

$$\frac{d^2V}{dz^2} - \rho\alpha_i V = 0 \qquad \text{for} \qquad z<z_0$$

$$\frac{d^2V}{dz^2} - \rho\alpha_e V = 0 \qquad \text{for} \qquad z>z_0 \tag{A2}$$

With the condition that V be continuous at z_0, the solution is

$$V = A\lambda_e/\lambda_i \sinh\lambda_i(z-z_0) \qquad \text{for} \qquad z<z_0$$

$$V = A\sinh\lambda_e(z-z_0) \qquad \text{for} \qquad z>z_0 \tag{A3}$$

where $\lambda_e = (\rho\alpha_e)^{1/2}$, $\lambda_i = (\rho\alpha_i)1/2$ and A is arbitrary. Current balance is achieved by requiring that ion and electron currents are equal. Thus

$$-\int_0^{z_0} \alpha_i V dz = \int_{z_0}^{N} \alpha_e V dz \tag{A4}$$

which, using Eq. (A3) yields the condition

$$\cosh\lambda_i z_0 = \cosh\lambda_e(N-z_0) \tag{A5}$$

$$z_0/N = 1/(1+\lambda_i/\lambda_e) = 1/[1+(\alpha_i/\alpha_e)^{1/2}] \tag{A6}$$

With $\alpha_e = 2.4\times10^{-6}$ mho and $\alpha_i = 2\times10^{-8}$ mho, $z_0/N = 0.92$. Thus, 8% of the chain floats above the plasma potential. For ram ions, with $\alpha_r = 10^{-8}$ mho, $z_0/N = 0.94$.

These results are unaffected by increasing the number of chains from one to M. With M chains, a factor of M would multiply both α_i And α_e in Eq. (A6), leaving it unchanged. Also, these results are rather insensitive to the exact values of the electron and ion conductances. For example, increasing α_i by a factor of two only reduces z_0/N to 89%.

Using the solution given in Eq. (A3) above, one can easily calculate the power loss to the plasma in floating equilibrium by integrating the loss per interconnect over the whole array. The result is:

$$P = A^2\lambda_e(\sinh(2N\bar{\lambda})/2 - N)/2$$

where

$$\bar{\lambda} = \lambda_e\lambda_i/(\lambda_e+\lambda_i)$$

With $N=1000$, $M=1500$, $A=1$ cm^2 and the above plasma conductances, this loss is 3.2% of the power produced by an array operating at 80% of maximum power.

Plasma Interaction Distribution

Let α be the fraction of an array whose plasma impedances, Z_p, are added together in parallel at the positive terminal, $V+$. Thus δ is the "plasma split" parameter of Sec. IV A. Let $\alpha = 1 - z_0/N$. Then the following lumped circuit elements obtain at the terminals in the mixed-case approximation.

1) Capacitance

$$C+ = \delta NMCp \qquad C- = (1-\delta)NMCp$$

2) Resistance

$$\text{for } \alpha <= \gamma,\ 1/R+ = \alpha NM\alpha_e$$

$$\text{and } 1/R- = NM[(\gamma-\delta)\alpha_e + (1-\gamma)\alpha_i]$$

$$\text{for } \delta >= \gamma,\ 1/R- = (1-\delta)NM\alpha_i$$

$$\text{and } 1/R+ = NM[\gamma\alpha_e + (\delta-\gamma)\alpha_i]$$

Appendix B

Circuit Analysis

The circuit of Fig. 3 obeys the following set of transient equations with initial conditions $v+(0)=v-(0)=0$:

$$a_1 dv_+/dt + a_2 v_+ - c dv_-/dt - f v_- = 0$$

$$b_1 dv_-/dt + b_2 v_- - c dv_+/dt - f v_+ = i_s(t) \qquad \text{(B1)}$$

where

$$a_1 = C_+ + C_0, \quad b_1 = C_- + C_0, \quad a_2 = 1/R_+ + 1/R_0$$

$$b_2 = 1/R_- + 1/R_0, \; c = C_0, \quad f = 1/R_0, \; R_0 = \rho_0 R_L/(\rho_0 + R_L)$$

$$p(s) = \mathcal{L} i_s(t) \text{ and } D = (b_1 s + b_2)\cdot(a_1 s + a_2) - (cs+f)^2 \qquad \text{(B2)}$$

Using the Laplace transform

$$q(s) = \mathcal{L} v(t) = \int_0^\infty e^{-st} v(t)\,dt$$

Eqs. (B1) form a pair of first order algebraic equations in the variable s. The solutions for $q+$ and $q-$ are

$$q_+(s) = p(s)\cdot(cs+f)/D \text{ and } q_-(s) = p(s)\cdot(a_1 s + a_2)/D$$

where

$$p(s) = \mathcal{L} i_s(t) \text{ and } D = (b_1 s + b_2)\cdot(a_1 s + a_2) - (cs+f)^2 \qquad \text{(B2)}$$

The denominator D may be put in the form, $D = A(s-\lambda_1)(s-\lambda_2)$, where $A = b_1 a_1 - c^2$ and the λ's are solutions of the equation, $D=0$. The transforms for $q+$ and $q-$ may be inverted using well-known theorems with the results

$$v+ = [1/A(\lambda_1 - \lambda_2)] \cdot \int_0^t [(c\lambda_1 + f)e^{\lambda_1 \tau} - (c\lambda_2 + f)e^{\lambda_2 \tau}]$$

$$\cdot i_s(t-\tau)\,d\tau \qquad \text{(B3)}$$

and $v-$ is the same but with c,f replaced by a_1,a_2 respectively. These are the solutions for arbitrary $i_s(t)$, provided $i_s(0)=0$. Let us take the special case

$$i_s(t) = I_0(e^{-t/T} - e^{-Kt/T}) \quad \text{for} \quad K>1 \qquad \text{(B4)}$$

Then, doing the integrals in Eq. (B3) gives

$$v_+(t) = [I_0/A]\cdot[B_1 e^{-tK/T} + B_2 e^{-t/T} + B_3 e^{\lambda_1 t} + B_4 e^{\lambda_2 t}]$$

where

$$B_1 = (cK/T - f)/[(\lambda_1 + K/T)\cdot(\lambda_2 + K/T)]$$

$$B_2 = -(c/T - f)/[(\lambda_1 + 1/T)\cdot(\lambda_1 + K/T)]$$

$$B_3 = (K-1)\cdot(c\lambda_1 + f)/[(\lambda_1 - \lambda_2)T(\lambda_1 + 1/T)(\lambda_1 + K/T)]$$

$$B_4 = -(K-1)\cdot(c\lambda_2 + f)$$

$$\div [(\lambda_1 - \lambda_2)T(\lambda_2 + 1/T)(\lambda_2 + K/T)] \qquad \text{(B5)}$$

The expression for $v-$ is identical but with the replacement of c,f by a_1,a_2. From v_+ and v_- one can easily construct the load transient, $v_+ - v_-$.

Let us consider a simple but useful limit to the above solutions. Suppose that the solar array internal capacitance, C_0, is so small that it can be neglected and that all the plasma impedance is at the positive terminal, i.e., $\delta = 1$. Then, with $C_- = 1/R_- = 0$ and the limit $C_0 \to 0$ taken last, one finds

$$v+(t) = I_0 R_+ T\{e^{-Kt/T}/(K\tau_+ - T) - e^{-t/T}/(\tau_+ - T)$$

$$+ (K-1)\tau_+ e^{-t/\tau_+}/[(\tau_+ - T)(K\tau_+ - T)]\} \qquad \text{(B6)}$$

and $v+(t) - v_-(t) = -I_0 R_0 (e^{-t/T} - e^{-Kt/T}) = -R_0 i_s(t)$ where $\tau_+ = R_+ C_+$. This expression for the load transient, $v_+ - v_-$, is to be expected since, with $C_0 = 0$, the arc current flows through a pure resistance, R_0. In actual practice, C_0 is quite small and Eqs. (B6) give a rough estimate of transient amplitudes.

VII. Acknowledgment

The author wishes to acknowledge gratefully the support of the NASA-Lewis Research Center, where he was a Visiting Scientist when this work was undertaken. The suggestions and comments of Drs. C.K. Purvis and D.B. Snyder, both of the Spacecraft Environment Section of the laboratory, were especially helpful.

References

[1]Stevens, N.J., "Review of Biased Solar Array-Plasma Interaction Studies," NASA TM 82693, 1981.

[2]Grier, N.T., "Dilute Plasma Coupling Currents to a High Voltage Solar Array in Weak Magnetic Fields," NASA TM 83687, 1984.

[3]Snyder, D.B., "Discharges on a Negatively Biased Solar Array in a Charged Particle Environment," NASA TM 83644, *Spacecraft Environmental Interactions Technology,* 1983, NASA-CP-2359, pp. 379-388.

[4]Leung, P., "Discharge Characteristics of a Simulated Solar Cell Array," *IEEE Transactions on Nuclear Science*, NS-30, 1983, pp. 4311-4315.

[5]Purvis, C.K. et al. "Interaction of Large, High Power Systems With Operational Orbit Charged Particle Environments," NASA TM 73867, 1977.

[6]Domitz, S. and Kolecki, J., "Effect of Plasma Currents on Solar-Array Power Output," *Spacecraft Charging Technology,* NASA-CP2071, 1978.

[7]Rauschenbach, H.S., *Solar Cell Array Design Handbook,* Van Nostrand Reinhold, New York, 1980, pp. 52-56.

[8]Smith, R.E. and West, G.S., *Space and Planetary Environment Criteria Guidelines for Use in Space Vehicle Development*, 1982 Revision, Vol. 1., NASA TM 82478.

[9]Chen, F.F., "Electric probes," *Plasma Diagnostic Techniques,* R.N. Huddlestone and S.L. Leonard, eds., Academic Press, New York, 1965, pp. 113-200.

[10]Parker, L.W., and Whipple, E.C., Jr., "Theory of a Satellite Electrostatic Probe," *Annals of Physics*, 44, 1967, pp. 126-161.